DORDT UNIVERSITY

Dordt Digital Collections

Faculty Work Comprehensive List

6-26-2020

Mapping Jupiter's Mischief

Channon Visscher
Dordt University, channon.visscher@dordt.edu

Follow this and additional works at: https://digitalcollections.dordt.edu/faculty_work

 Part of the Astrophysics and Astronomy Commons

Recommended Citation

Visscher, C. (2020). Mapping Jupiter's Mischief. *JGR Planets, 125* (8) https://doi.org/10.1029/2020JE006526

This Article is brought to you for free and open access by Dordt Digital Collections. It has been accepted for inclusion in Faculty Work Comprehensive List by an authorized administrator of Dordt Digital Collections. For more information, please contact ingrid.mulder@dordt.edu.

Mapping Jupiter's Mischief

Abstract

New results (Grassi et al., 2020, https://doi.org/10.1029/2019JE006206) from analysis of Juno Jovian Infrared Auroral Mapper (JIRAM) 4- to 5-μm observations provide updated latitudinal abundance profiles and measurements of the spatial distribution of H2O, NH3, PH3, GeH4, and AsH3 in Jupiter's troposphere near the 3- to 5-bar level. The observed compositional variations provide new constraints on processes shaping chemical abundances in the cloud-forming region of the troposphere, including vertical and horizontal atmospheric mixing, meteorology and cloud formation, transport-induced quenching, and photochemistry. Along with recent results from the Juno Microwave Radiometer (MWR) for NH3 and H2O abundances far below the clouds, the JIRAM measurements of key disequilibrium tracer species can also be used to explore the coupled dynamics, chemistry, and bulk composition of Jupiter's deep atmosphere. The heavy element abundance inventory on Jupiter is a key constraint for the development and assessment of giant planet formation models. Combined with prior ground-based, spacecraft, and in situ observations, the Juno results suggest near-uniform (~2–4 times) enhancements over protosolar abundances for several heavy elements in Jupiter's atmosphere, giving new clues about the composition of the material accreted, the timing and location of formation, and the internal evolution of Jupiter over the history of the solar system.

Keywords

Jupiter, Juno, planetary formation, atmospheric chemistry

Disciplines

Astrophysics and Astronomy

This article is available at Dordt Digital Collections: https://digitalcollections.dordt.edu/faculty_work/1343

Check for updates

JGR Planets

COMMENTARY
10.1029/2020JE006526

Special Section:
Jupiter Midway Through the Juno Mission

Mapping Jupiter's Mischief

Channon Visscher[1,2]

[1]Chemistry & Planetary Sciences, Dordt University, Sioux Center, IA, USA, [2]Space Science Institute, Boulder, CO, USA

Abstract New results (Grassi et al., 2020, https://doi.org/10.1029/2019JE006206) from analysis of *Juno* Jovian Infrared Auroral Mapper (JIRAM) 4- to 5-μm observations provide updated latitudinal abundance profiles and measurements of the spatial distribution of H_2O, NH_3, PH_3, GeH_4, and AsH_3 in Jupiter's troposphere near the 3- to 5-bar level. The observed compositional variations provide new constraints on processes shaping chemical abundances in the cloud-forming region of the troposphere, including vertical and horizontal atmospheric mixing, meteorology and cloud formation, transport-induced quenching, and photochemistry. Along with recent results from the *Juno* Microwave Radiometer (MWR) for NH_3 and H_2O abundances far below the clouds, the JIRAM measurements of key disequilibrium tracer species can also be used to explore the coupled dynamics, chemistry, and bulk composition of Jupiter's deep atmosphere. The heavy element abundance inventory on Jupiter is a key constraint for the development and assessment of giant planet formation models. Combined with prior ground-based, spacecraft, and in situ observations, the *Juno* results suggest near-uniform (~2–4 times) enhancements over protosolar abundances for several heavy elements in Jupiter's atmosphere, giving new clues about the composition of the material accreted, the timing and location of formation, and the internal evolution of Jupiter over the history of the solar system.

Plain Language Summary New results from the *Juno* spacecraft provide high-resolution measurements of the distribution of several key gases in Jupiter's atmosphere and show how their abundances vary with latitude. The observed abundance distributions result from a complex tangle of chemical and physical processes, including atmospheric circulation, chemical reactions, and cloud formation that together shape the abundances of chemical species in the troposphere. Recent infrared and microwave measurements also provide key clues about the chemistry and composition of Jupiter's atmosphere below the clouds and into the deep interior. The new results from the *Juno* mission thus represent a major step toward completing its goal of providing an accurate elemental inventory of Jupiter's deep atmosphere and deliver new insights into Jupiter's formation and chemical evolution: What is Jupiter made of and how did it get that way?

Key Points:
- Recent Juno results provide updated latitudinal abundance profiles that map the distribution of several key atmospheric species on Jupiter
- Mapping key gases in Jupiter's troposphere characterizes the chemical and dynamical processes responsible for Jupiter's banded appearance
- Chemistry in Jupiter's troposphere is tied to element abundances in the deep atmosphere, providing constraints for Jovian formation models

Correspondence to:
C. Visscher,
channon.visscher@dordt.edu

Citation:
Visscher, C. (2020). Mapping Jupiter's mischief. *Journal of Geophysical Research: Planets*, *125*, e2020JE006526. https://doi.org/10.1029/2020JE006526

Received 14 MAY 2020
Accepted 18 JUN 2020
Accepted article online 26 JUN 2020

©2020. American Geophysical Union. All Rights Reserved.

1. Prelude to *Juno*

Jupiter is the most massive planet in the solar system and played a central role in shaping the formation history, architecture, and composition of the planets. Important clues about early planetary history can thus be found in our understanding of Jupiter's structure and chemical composition. For example, Jupiter consists mostly of hydrogen with a bulk composition roughly similar to that of the Sun, suggesting that Jupiter (and other H-rich giant planets) formed while there was still enough H and He gas in the protoplanetary disk available for significant accretion (for reviews, see Lunine et al., 2004; Taylor et al., 2004). Moreover, observations of exoplanetary systems showing evidence of planetary migration, along with modern dynamical models, suggest that Jupiter drove planetesimal migration and accretion throughout the early solar system (e.g., see D'Angelo & Lissauer, 2018; Gomes et al., 2005; Helled et al., 2014; Raymond et al., 2018; Tsiganis et al., 2005, and references therein). Jupiter thus provides a record of the formation and earliest evolution of our own planetary system and serves as a prototype for similar formation processes in exoplanetary systems.

Theoretical models and infrared observations also show that Jupiter emits nearly twice as much energy as it absorbs from the Sun, suggesting a hot, convective interior. For this reason, gas abundances in the troposphere of Jupiter have generally been considered (while accounting for cloud formation) indicative of its bulk composition. A key constraint for Jovian formation models is thus the comparison of model results to the observed abundances of compounds such as CH_4, NH_3, H_2S, and H_2O, taken to represent the planetary elemental abundances of the "heavy elements" C, N, S, and the majority of planetary O, respectively.

Figure 1. Jupiter near 56°N as seen by *Juno* from a distance of 15,500 km during its thirteenth perijove encounter. The bright clouds are inferred to be high clouds of NH_3, with darker cloud material located deeper in the atmosphere. JunoCam visible light image with colors exaggerated. Image credit: NASA/JPL-Caltech/SwRI/MSSS/Gerald Eichstdt/Sen Doran (CC NC SA).

For example, in situ measurements of Jupiter's troposphere by the *Galileo* Probe Mass Spectrometer (GPMS; e.g., Mahaffy et al., 2000; Wong et al., 2004) showed enhancements in heavy-element-to-H_2 ratios for several elements (C, N, S, Ar, Kr, and Xe) and depletions in others (e.g., Ne and O) relative to the original (or "protosolar") element inventory of the solar system. In this context, the success of planetary formation and evolution models are measured by their ability to reproduce the observed enrichments and/or depletions. An accurate determination of Jupiter's global element inventory has thus become a major goal of planetary research.

However, efforts to determine some representative Jovian composition have posed a challenging task. Jupiter is not a *tame* planet. High clouds of icy NH_3 or storm-driven H_2O clouds obscure deeper atmospheric levels (e.g., see Figure 1). And recent observations suggest an atmosphere as variable and tumultuous as the swirling clouds suggest (e.g., Antuñano et al., 2019; Bolton et al., 2017; de Pater et al., 2016; Fletcher, 2017, 2020; Li et al., 2017). Although the *Galileo* Probe provided crucial measurements of Jupiter's troposphere, it descended into an anomalously dry "hot spot" region (features found along the boundary between the equatorial zone and the north equatorial belt) characterized by low cloud opacity, low abundances of cloud-forming species, high thermal (5-μm) emission, and a water abundance that was still increasing with depth when the probe signal was lost at the 22-bar level (e.g., Niemann et al., 1998; Orton et al., 1998; Wong et al., 2004). So the question remained to what extent the GPMS results for H_2O could be taken as representative of some deep, well-mixed oxygen inventory for Jupiter as a whole. The *Juno* mission was designed to remotely sound the deep atmosphere to hundreds of bars, far beneath the upper veil of clouds, to address such global questions about Jupiter's interior structure and bulk composition—and, in turn, its formation and chemical evolution.

2. *Juno* at Jupiter

Launched in the summer of 2011, *Juno* entered an eccentric polar orbit of Jupiter in the summer of 2016, swooping closely past the planet (less than 5,000 km above the cloud tops) every 53.5 days. The major scientific products of these encounters are now coming to light. New results by Grassi et al. (2020) map the distribution of key atmospheric gases in Jupiter's atmosphere using data collected by the Jovian Infrared Auroral Mapper (JIRAM) over the first 2 years of *Juno*'s orbit (August 2016 to September 2018). The JIRAM observations at 4–5 μm are sensitive to thermal emission from the cloud-forming region near ~3–5 bar (with clouds in silhouette against a bright background), along with spectral features from several tropospheric gases. Grassi et al. (2020) performed retrieval analysis on a subset of available JIRAM data, using spectra selected for relatively high radiance, low emission angle, and high resolution. The *Juno* spacecraft measurements provide two key advantages over previous observations: very high resolution (courtesy of its close proximity to Jupiter) and coverage at high latitudes using similar viewing geometries as for low latitudes (courtesy of its polar orbit).

Grassi et al. (2020) provide new latitudinal abundance profiles (summarized in Figure 2) and map the distribution of H_2O, NH_3, PH_3, GeH_4, and AsH_3 in the cloud-forming region of Jupiter's troposphere. The results also allow for new analysis of persistent correlations of gas abundances within discrete regions on Jupiter (e.g., belts and polar regions) and—in the case of water vapor relative humidity—possible associations with zonal wind patterns (Grassi et al., 2020). The observed tropospheric abundances result from a tangle of closely coupled chemical, dynamical, and radiative processes, including vertical and horizontal mixing, meteorology and cloud formation, thermochemical kinetics and disequilibrium, and photochemistry. The *Juno* results thus provide new constraints for a range of models exploring how such processes conspire to shape the chemical composition of Jupiter's troposphere. The new results also represent another major step toward

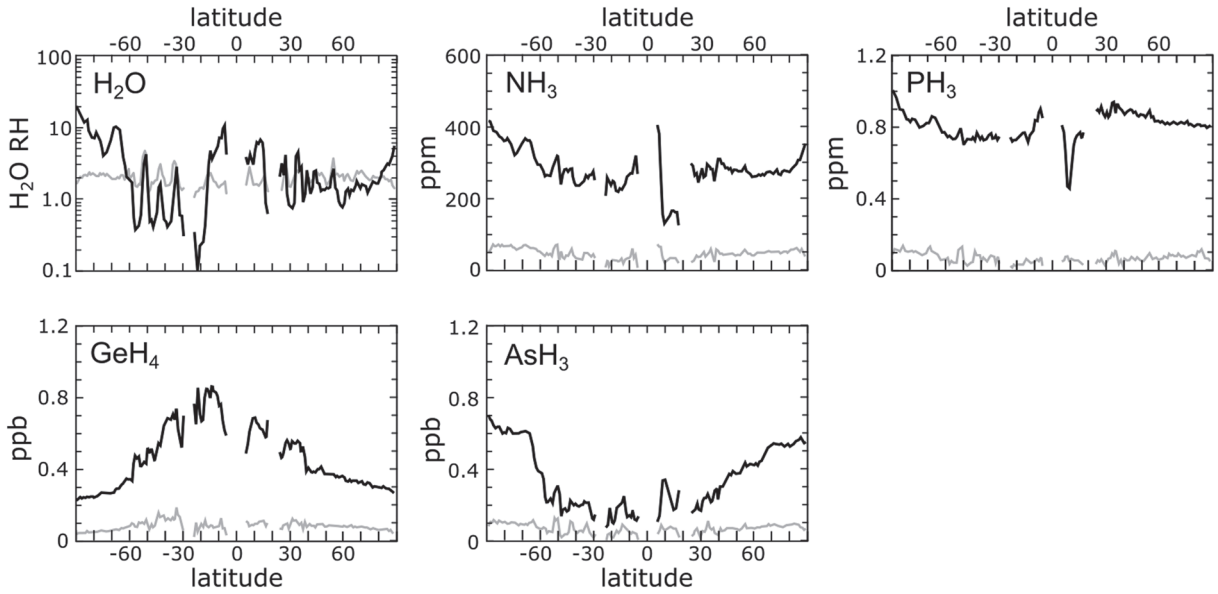

Figure 2. Averaged latitudinal profiles for H_2O (relative humidity), NH_3, PH_3, GeH_4, and AsH_3 (mole fractions) from Grassi et al. (2020) using *Juno* JIRAM observations from the first 15 perijove encounters (PJ1–PJ15). The black curves represent mean abundance values, and the gray curves represent the standard deviation over all PJ1–PJ15 profiles. Gaps in the abundance profiles occur at latitudes with high aerosol opacity (corresponding with cloud-thick zones), where measurements of the gas composition are difficult to obtain. See Grassi et al. (2020) for details.

completing *Juno's* goal of mapping key species (including disequilibrium species) to provide an accurate elemental inventory of Jupiter's deep atmosphere.

3. Chemical Connections to the Deep

A number of the minor species observed in Jupiter's troposphere (including CO, PH_3, GeH_4, and AsH_3) are present in abundances that far exceed those expected from thermodynamic equilibrium. As was first demonstrated for CO (Prinn & Barshay, 1977), this behavior represents vertical mixing from deeper, denser, warmer levels where the species in question has a higher abundance at an equilibrium maintained by fast reaction kinetics (i.e., chemical timescales are short relative to mixing timescales, $\tau_{chem}\tau_{mix}$). However, departures from equilibrium can occur at higher, cooler altitudes where convective vertical mixing occurs faster than chemical reactions can maintain equilibrium (i.e., $\tau_{chem} > \tau_{mix}$), effectively "quenching" the abundance of a molecular species at a fixed value throughout the upper troposphere. For most disequilibrium species, the "quench level" for this transition (i.e., $\tau_{chem} \approx \tau_{mix}$) is typically near 600–1000 K (Fegley & Lodders, 1994; Fegley & Prinn, 1985; Visscher & Moses, 2011; Wang et al., 2016). The observed tropospheric abundances of tracer species such as CO, PH_3, GeH_4, and AsH_3 thus provide a window to the dynamics, chemistry, and composition of Jupiter's deep atmosphere down to approximately kilobar levels (e.g., Giles, Fletcher, & Irwin, 2017; Grassi et al., 2020).

For example, PH_3 is expected to be the dominant P-bearing phase at high temperatures in Jupiter's deep atmosphere but is subject to removal by oxidation and/or condensation at lower temperatures (<500 K). There has been some debate regarding the identity of the lower temperature P-bearing phase, mostly due differences in thermodynamic data adopted for phosphorus oxides such as P_4O_6 (for discussion, see Fegley & Lodders, 1994), and various compounds have been considered to replace PH_3 at lower temperatures, including: P_4O_6 (Fegley & Lodders, 1994; Visscher et al., 2006), P_4O_{10} (Borunov et al., 1995), H_3PO_4 (Wang et al., 2016), and/or $NH_4H_2PO_4$ (Fegley & Lodders, 1994; Morley et al., 2018; Visscher et al., 2006). In any case, there is consensus that disequilibrium PH_3 observed in the troposphere comes from a deep atmospheric source representative of Jupiter's elemental P inventory. However, the observed PH_3 abundance—possibly including the deep abundance—varies as a function of latitude in both 5 μm (e.g., Drossart et al., 1990; Giles et al., 2015; Giles, Fletcher, & Irwin, 2017; Grassi et al., 2020) and midinfrared

(e.g., Fletcher et al., 2009, 2016; Irwin et al., 2004) observations. Notably, midinfrared PH_3 values have typically been ~2 times higher than the 5-μm values and show an equatorial maximum as high as ~2-ppm PH_3 (e.g., see Fletcher et al., 2009, 2016) in the same location as the NH_3 maximum (de Pater et al., 2016; Li et al., 2017). Both PH_3 and NH_3 also show minima near 10°N in the JIRAM data (see Figure 2), suggestive of similar dynamical influences. Adopting the ~1-ppm PH_3 abundance maximum observed by JIRAM (near the south pole, see Figure 2 Grassi et al., 2020) as a lower limit for the deep PH_3 abundance yields a Jovian phosphorus inventory of at least 1.3 times the protosolar value.

Germane (GeH_4) is also subject to removal by condensation at temperatures below 700 K yet survives at approximately ppb disequilibrium concentrations into Jupiter's upper troposphere. Because Ge is distributed among several Ge-bearing species at high temperatures (Fegley & Lodders, 1994), GeH_4 cannot be taken as representative of Jupiter's bulk Ge inventory (note that 1-ppb GeH_4 corresponds to 0.1 times the protosolar Ge abundance). Nevertheless, quenched GeH_4 is expected to show strong sensitivity to the convective mixing rate compared to PH_3 or AsH_3 (Fegley & Lodders, 1994; Fegley & Prinn, 1985; Wang et al., 2016). Noting that convective mixing will be stronger at low latitudes on a rotating planet such as Jupiter (Flasar & Gierasch, 1977; Visscher et al., 2010), Wang et al. (2016) demonstrated that higher GeH_4 abundances would be expected near the equator than near the poles, in agreement with the latitudinal trends observed by JIRAM (e.g., see Figure 2 and Giles, Fletcher, & Irwin, 2017; Grassi et al., 2020, for discussion and comparison of observed trends).

On the other hand, the AsH_3 abundance is expected to be less sensitive to the rate of mixing (Fegley & Lodders, 1994; Wang et al., 2016) and the latitudinal profile of tropospheric AsH_3 is enigmatic, with an abundance that *increases* toward the poles (see Figure 2; Giles, Fletcher, & Irwin, 2017; Grassi et al., 2020). Although the chemical scale height for each disequilibrium species differs depending upon reaction kinetics and quench conditions, each is presumably subject to the same convective transport. The unexpected AsH_3 profile thus suggests that the chemical processes shaping the AsH_3 abundance remain incompletely understood. As suggested by Giles, Fletcher, and Irwin (2017), the observed distribution is plausibly explained by photolytic destruction of AsH_3 in Jupiter's upper troposphere (analogous to NH_3 and PH_3 photochemistry near 200 mbar Kaye & Strobel, 1983; Strobel, 1977), where higher photolysis rates toward the equator yield less AsH_3. Assuming that AsH_3 is the dominant As bearing in Jupiter's deep atmosphere (Fegley & Lodders, 1994), the maximum AsH_3 abundance of 0.7 ppb measured by Grassi et al. (2020) suggests an enhancement of ~1.3 times the protosolar value, similar to that observed for PH_3.

Jupiter's deep atmospheric water abundance (and more generally, Jupiter's oxygen inventory) is critical to our understanding of Jupiter's formation as well as dynamical and chemical processes (such as cloud formation) in Jupiter's troposphere. Prior to *Juno*, however, the obscuring presence of clouds and other opacity sources has long limited our ability to determine the H_2O abundance below the clouds. Earth-based infrared observations must contend with telluric H_2O contamination (e.g., see Bjoraker et al., 2016, 2018), whereas centimeter measurements must account for synchroton emission from Jupiter's radiation belts (e.g., de Pater et al., 2016). Moreover, as noted above, it is unclear to what extent near-infrared observations (most sensitive to hot spot regions) or the GPMS measurement ($X_{H_2O} = 420 \pm 140$ ppm, corresponding to ~0.5 times the protosolar H_2O/H_2 ratio) can be taken as representative of the bulk planetary inventory. (For reference, a "protosolar" atmospheric water abundance is defined here as $X_{H_2O} = 830$ ppm or $X_{H_2O}/X_{H_2} = 9.61 \times 10^{-4}$ using elemental abundances from Lodders (2010) and accounting for the removal of some oxygen into rock (e.g., Visscher et al., 2010). For conversion between mole fraction abundances and element-to-H_2 mixing ratios on Jupiter, a hydrogen abundance of $X_{H_2} = 0.864$ is adopted based upon *Galileo* measurements of the He abundance (Niemann et al., 1998; von Zahn et al., 1998).)

Given these challenges, several investigators turned to chemical models to estimate the H_2O abundance by considering how water in the deep atmosphere influences the observed behavior of other species (in particular CO) mixed into the upper troposphere. For example, the ~1-ppb CO observed in Jupiter's troposphere (e.g., Bézard et al., 2002; Bjoraker et al., 2018) is far greater (over 20 orders of magnitude) than the equilibrium abundance predicted near the 6-bar level, suggesting rapid vertical mixing from deeper in the atmosphere where CO is more abundant and forms via net reactions such as $CH_4 + H_2O \rightleftarrows CO + 3H_2$. For a given carbon inventory (characterized by CH_4), the observed (quenched) abundance of CO thus depends

upon the rate of reactions that interconvert CO $\rightleftarrows$ CH_4, the strength of convective vertical transport, and the abundance of water in the deep atmosphere: More H_2O yields more CO.

Following the approach pioneered by Prinn and Barshay (1977) and Fegley and Prinn (1988), modern numerical studies of H-C-O chemistry in Jupiter's atmosphere use extensive reaction networks to estimate the H_2O abundance based upon CO quench kinetics (e.g., see Visscher et al., 2010; Visscher & Moses 2011, who estimated 420–2,160-ppm H_2O). More recently, Wang et al. (2015) showed that for a narrower range of rapid mixing rates expected near equatorial latitudes, the kinetic schemes of Visscher and Moses (2011) and Venot et al. (2012) give 85- to 640-ppm H_2O and 2,500- to 9,300-ppm H_2O, respectively. Full resolution of model differences (caused by differences in adopted rates of key reactions in the CO $\rightleftarrows$ CH_4 reaction scheme) may require improved understanding of the dynamical behavior of Jupiter's deep atmosphere and/or new studies that explore whether the reaction networks adapted from H-C-O combustion experiments under oxidizing conditions will behave consistently in hydrogen-rich planetary environments (e.g., see Moses, 2014; Moses et al., 2011; Venot et al., 2012, 2020; Wang et al., 2015, for further discussion). In the meantime, chemical models of the deep atmosphere will also be improved by new observational constraints on Jupiter's composition far below the clouds.

4. Looking Below the Clouds

The spatial distribution of cloud-forming species such as NH_3 and H_2O mapped by JIRAM provide information about the meteorological processes that affect their abundances in the cloud-forming region of Jupiter's troposphere ($\lesssim$ 10 bar). For example, the observed H_2Orelative humidity is highly variable with latitude (see Figure 2), with local enhancements in water vapor that appear to be associated with cyclonic regions consistent with models of moist convection (e.g., see Dowling & Gierasch, 1989; Fletcher et al., 2017; Giles et al., 2015; Grassi et al., 2020; Ingersoll et al., 2004; Roos-Serote et al., 2000). The distribution of NH_3 likewise shows abundance variations (see Figure 2) shaped by vertical and horizontal mixing, including an enhancement along the edges of the equatorial zone, a strong depletion near 10°N (consistent with microwave measurements; see Li et al., 2017, and discussion below), and longitudinal variations (including NH_3-rich plumes) near hot spot latitudes (e.g., see de Pater et al., 2016; Fletcher et al., 2016, 2020; Giles, Fletcher, Irwin, Orton, & Sinclair, 2017; Grassi et al., 2020; Li et al., 2017).

While the JIRAM results provide new abundance estimates in the cloud-forming region of Jupiter's atmosphere, recent results from *Juno* Microwave Radiometer (MWR) measurements provide complementary estimates of the NH_3 and H_2O abundances well below the clouds (e.g., see Janssen et al., 2017). Because NH_3 absorbs more strongly than H_2O, MWR determinations of the water abundance require an accurate estimate of the NH_3 abundance profile, which is best constrained in the equatorial zone (e.g., Li et al., 2017). Using this approach (for 351-ppm NH_3 or 2.5 times protosolar N), Li et al. (2020) obtain a deep H_2O abundance of $2,500^{+2,200}_{-1,600}$ ppm (or $3.0^{+2.6}_{-1.9}$ times protosolar H_2O) in the equatorial zone, confirming that the GPMS measurement (420 ppm) was not representative of Jupiter's deep water inventory. Combined with prior ground-based, spacecraft, and in situ observations, the *Juno* results thus suggest roughly uniform (∼2–4 times) enhancements over protosolar abundances for several heavy elements in Jupiter's atmosphere.

The deep abundance measurements of the major cloud-forming species (Li et al., 2020) along with disequilibrium abundances (Grassi et al., 2020) can also be used to identify connections between the upper troposphere and the deep atmosphere and to explore related questions about which chemical pathways, atmospheric motions, and meteorological processes are shaping the observed abundances of tropospheric chemical species: How deep does chemical variability extend? To what extent do deep atmospheric abundances represent bulk element inventories? For example, the MWR results show spatial variations in NH_3 extending to at least the ∼50-bar level (e.g., see Bolton et al., 2017; Ingersoll et al., 2017; Li et al., 2017) with a deep abundance (∼360 ppm) less than that observed by GPMS (570 ppm Wong et al., 2004). In addition, high-resolution *Juno* measurements of Jupiter's gravity field suggest the presence of a diluted core and the possibility that the heavy element inventory is not uniformly mixed throughout the planet as a whole (e.g., see Debras & Chabrier, 2019; Wahl et al., 2017), presenting new challenges for inferring the chemical consequences of Jupiter's atmospheric evolution.

Nevertheless, the observed Jovian water inventory provides a key constraint on the composition of the material accreted, the timing and location of formation, and the internal chemical and structural evolution of Jupiter over the history of the solar system. A bulk oxygen inventory similar to that of other heavy elements (as suggested by *Juno* MWR results) calls into question formation scenarios that predict either very large or very small water abundances, whereas models that predict roughly similar heavy-element enhancements invite a closer look (e.g., see Guillot & Hueso, 2006; Lodders, 2004; Mousis et al., 2019; Owen et al., 1999; Wong et al., 2008, for references and further discussion). The new results also raise ongoing questions about core-accretion and gravitational collapse during giant planet formation: Should we consider Jupiter to be uniformly *enriched* in heavy elements? Or instead *depleted* in H and He? Our understanding of giant planet formation within an evolving protoplanetary disk—informed by ongoing ground-based and *Juno* observations of key species in Jupiter's troposphere—will continue shape how these questions are addressed both inside and outside of our own planetary system.

Data Availability Statement

No new data were generated in the preparation of this manuscript. Data used for the abundance profiles in Figure 2 are included in Grassi et al. (2020), and the full JIRAM data sets can be found in Grassi (2019).

Acknowledgments

I thank the two anonymous reviewers for their reviews and many constructive suggestions that were incorporated into the commentary.

References

Antuñano, A., Fletcher, L. N., Orton, G. S., Melin, H., Milan, S., Rogers, J., et al. (2019). Jupiter's atmospheric variability from long-term ground-based observations at 5 μm. *Astronomical Journal*, *158*(3), 130. https://doi.org/10.3847/1538-3881/ab2cd6

Bézard, B., Lellouch, E., Strobel, D., Maillard, J.-P., & Drossart, P. (2002). Carbon monoxide on Jupiter: Evidence for both internal and external sources. *Icarus*, *159*(1), 95–111. https://doi.org/10.1006/icar.2002.6917

Bjoraker, G. L., de Pater, I., Wong, M. H., Adamkovics, M., Hewagama, T., & Hesman, B. (2016). Volatile abundances and the deep cloud structure in Jupiter's Great Red Spot. *Bulletin of the American Astronomical Society (DPS)*, *48*(7), 508.05.

Bjoraker, G. L., Wong, M. H., de Pater, I., Hewagama, T., Ádámkovics, M., & Orton, G. S. (2018). The gas composition and deep cloud structure of Jupiter's Great Red Spot. *Astronomical Journal*, *156*(3), 101. https://doi.org/10.3847/1538-3881/aad186

Bolton, S. J., Adriani, A., Adumitroaie, V., Allison, M., Anderson, J., Atreya, S., et al. (2017). Jupiter's interior and deep atmosphere: The initial pole-to-pole passes with the Juno spacecraft. *Science*, *356*(6340), 821–825. https://doi.org/10.1126/science.aal2108

Borunov, S., Dorofeeva, V., Khodakovsky, I., Drossart, P., Lellouch, E., & Encrenaz, T. (1995). Phosphorus chemistry in atmosphere of Jupiter: A reassessment. *Icarus*, *113*, 460–464. https://doi.org/10.1006/icar.1995.1036

D'Angelo, G., & Lissauer, J. J. (2018). Formation of giant planets. In H. Deeg & J. Belmont (Eds), *Handbook of exoplanets* (pp. 140). Cham: Springer. https://doi.org/10.1007/978-3-319-55333-7_140

de Pater, I., Sault, R. J., Butler, B., DeBoer, D., & Wong, M. H. (2016). Peering through Jupiter's clouds with radio spectral imaging. *Science*, *352*(6290), 1198–1201. https://doi.org/10.1126/science.aaf2210

Debras, F., & Chabrier, G. (2019). New models of Jupiter in the context of Juno and Galileo. *Astrophysical Journal*, *872*(1), 100. https://doi.org/10.3847/1538-4357/aaff65

Dowling, T. E., & Gierasch, P. J. (1989). Cyclones and moist convection on Jovian planets. *Bulletin of the American Astronomical Society*, *21*, 946.

Drossart, P., Lellouch, E., Bezard, B., Maillard, J. P., & Tarrogo, G. (1990). Jupiter: Evidence for a phosphine enhancement at high northern latitudes. *Icarus*, *83*(1), 248–253. https://doi.org/10.1016/0019-1035(90)90018-5

Fegley, B., & Lodders, K. (1994). Chemical models of the deep atmospheres of Jupiter and Saturn. *Icarus*, *110*, 117–154. https://doi.org/10.1006/icar.1994.1111

Fegley, B., & Prinn, R. G. (1985). Equilibrium and nonequilibrium chemistry of Saturn's atmosphere - Implications for the observability of PH_3, N_2, CO, and GeH_4. *Astrophysical Journal*, *299*, 1067–1078. https://doi.org/10.1086/163775

Fegley, B., & Prinn, R. G. (1988). Chemical constraints on the water and total oxygen abundances in the deep atmosphere of Jupiter. *Astrophysical Journal*, *324*, 621–625. https://doi.org/10.1086/165922

Flasar, F. M., & Gierasch, P. J. (1977). Eddy diffusivities within Jupiter. In A. V. Jones (Ed.), *Planetary atmospheres* (pp. 85), *Proceedings of the Nineteenth Symposium of the Royal Society of Canada*. Ottawa: Royal Society of Canada.

Fletcher, L. N. (2017). Cycles of activity in the Jovian atmosphere. *Geophysical Research Letters*, *44*, 4725–4729. https://doi.org/10.1002/2017GL073806

Fletcher, L. N., Greathouse, T. K., Orton, G. S., Sinclair, J. A., Giles, R. S., Irwin, P. G. J., & Encrenaz, T. (2016). Mid-infrared mapping of Jupiter's temperatures, aerosol opacity and chemical distributions with IRTF/TEXES. *Icarus*, *278*, 128–161. https://doi.org/10.1016/j.icarus.2016.06.008

Fletcher, L. N., Orton, G. S., Greathouse, T. K., Rogers, J. H., Zhang, Z., Oyafuso, F. A., et al. (2020). Jupiter's equatorial plumes and hot spots: Spectral mapping from Gemini/TEXES and Juno/MWR. *arXiv e-prints*. arXiv:2004.00072.

Fletcher, L. N., Orton, G. S., Rogers, J. H., Giles, R. S., Payne, A. V., Irwin, P. G. J., & Vedovato, M. (2017). Moist convection and the 2010–2011 revival of Jupiter's South Equatorial Belt. *Icarus*, *286*, 94–117. https://doi.org/10.1016/j.icarus.2017.01.001

Fletcher, L. N., Orton, G. S., Teanby, N. A., & Irwin, P. G. J. (2009). Phosphine on Jupiter and Saturn from Cassini/CIRS. *Icarus*, *202*(2), 543–564. https://doi.org/10.1016/j.icarus.2009.03.023

Giles, R. S., Fletcher, L. N., & Irwin, P. G. J. (2015). Cloud structure and composition of Jupiter's troposphere from 5-μm Cassini VIMS spectroscopy. *Icarus*, *257*, 457–470. https://doi.org/10.1016/j.icarus.2015.05.030

Giles, R. S., Fletcher, L. N., & Irwin, P. G. J. (2017). Latitudinal variability in Jupiter's tropospheric disequilibrium species: GeH_4, AsH_3 and PH_3. *Icarus*, *289*, 254–269. https://doi.org/10.1016/j.icarus.2016.10.023

Giles, R. S., Fletcher, L. N., Irwin, P. G. J., Orton, G. S., & Sinclair, J. A. (2017). Ammonia in Jupiter's troposphere from high-resolution 5μm spectroscopy. *Geophysical Research Letters*, *44*, 10,838–10,844. https://doi.org/10.1002/2017GL075221

Gomes, R., Levison, H. F., Tsiganis, K., & Morbidelli, A. (2005). Origin of the cataclysmic Late Heavy Bombardment period of the terrestrial planets. *Nature*, *435*(7041), 466–469. https://doi.org/10.1038/nature03676

Grassi, D. (2019). Content of minor species in Jupiters upper troposphere as inferred from Juno JIRAM data (PJ1-15). Mendeley Data, v1. https://doi.org/10.17632/cjs32jv68g.1

Grassi, D., Adriani, A., Mura, A., Atreya, S. K., Fletcher, L. N., Lunine, J. I., et al. (2020). On the spatial distribution of minor species in Jupiter's troposphere as inferred from Juno JIRAM data. *Journal of Geophysical Research: Planets*, *125*, e2019JE006206. https://doi.org/10.1029/2019JE006206

Guillot, T., & Hueso, R. (2006). The composition of Jupiter: Sign of a (relatively) late formation in a chemically evolved protosolar disc. *Monthly Notices of the Royal Astronomical Society*, *367*(1), L47–L51. https://doi.org/10.1111/j.1745-3933.2006.00137.x

Helled, R., Bodenheimer, P., Podolak, M., Boley, A., Meru, F., Nayakshin, S., et al. (2014). Giant planet formation, evolution, and internal structure. In H. Beuther, R. S. Klessen, C. P. Dullemond, & T. Henning (Eds.), *Protostars and planets VI* (pp. 643). https://doi.org/10.2458/azu_uapress_9780816531240-ch028

Ingersoll, A. P., Adumitroaie, V., Allison, M. D., Atreya, S., Bellotti, A. A., Bolton, S. J., et al. (2017). Implications of the ammonia distribution on Jupiter from 1 to 100 bars as measured by the Juno Microwave Radiometer. *Geophysical Research Letters*, *44*, 7676–7685. https://doi.org/10.1002/2017GL074277

Ingersoll, A. P., Dowling, T. E., Gierasch, P. J., Orton, G. S., Read, P. L., Sánchez-Lavega, A., et al. (2004). Dynamics of Jupiter's atmosphere. In F. Bagenal, T. E. Dowling, & W. B. McKinnon (Eds.), *Jupiter. The planet, satellites and magnetosphere* (pp. 105–128). Cambridge: Cambridge University Press.

Irwin, P. G. J., Parrish, P., Fouchet, T., Calcutt, S. B., Taylor, F. W., Simon-Miller, A. A., & Nixon, C. A. (2004). Retrievals of Jovian tropospheric phosphine from Cassini/CIRS. *Icarus*, *172*, 37–49. https://doi.org/10.1016/j.icarus.2003.09.027

Janssen, M. A., Oswald, J. E., Brown, S. T., Gulkis, S., Levin, S. M., Bolton, S. J., et al. (2017). MWR: Microwave Radiometer for the Juno mission to Jupiter. *Space Science Reviews*, *213*(1-4), 139–185. https://doi.org/10.1007/s11214-017-0349-5

Kaye, J. A., & Strobel, D. F. (1983). HCN formation on Jupiter: The coupled photochemistry of ammonia and acetylene. *Icarus*, *54*(3), 417–433. https://doi.org/10.1016/0019-1035(83)90238-5

Li, C., Ingersoll, A., Bolton, S., Levin, S., Janssen, M., Atreya, S., et al. (2020). The water abundance in Jupiter's equatorial zone. *Nature Astronomy*, *4*, 609–616. https://doi.org/10.1038/s41550-020-1009-3

Li, C., Ingersoll, A., Janssen, M., Levin, S., Bolton, S., Adumitroaie, V., et al. (2017). The distribution of ammonia on Jupiter from a preliminary inversion of Juno microwave radiometer data. *Geophysical Research Letters*, *44*, 5317–5325. https://doi.org/10.1002/2017GL073159

Lodders, K. (2004). Jupiter formed with more tar than ice. *Astrophysical Journal*, *611*, 587–597. https://doi.org/10.1086/421970

Lodders, K. (2010). Solar system abundances of the elements. *Astrophysics and Space Science Proceedings*, *16*, 379. https://doi.org/10.1007/978-3-642-10352-0_8

Lunine, J. I., Coradini, A., Gautier, D., Owen, T. C., & Wuchterl, G. (2004). The origin of Jupiter. In *Jupiter. The planet, satellites and magnetosphere* (pp. 19–34).

Mahaffy, P. R., Niemann, H. B., Alpert, A., Atreya, S. K., Demick, J., Donahue, T. M., et al. (2000). Noble gas abundance and isotope ratios in the atmosphere of Jupiter from the Galileo Probe Mass Spectrometer. *Journal of Geophysical Research*, *105*, 15,061–15,072. https://doi.org/10.1029/1999JE001224

Morley, C. V., Skemer, A. J., Allers, K. N., Marley, M. S., Faherty, J. K., Visscher, C., et al. (2018). An L band spectrum of the coldest brown dwarf. *Astrophysical Journal*, *858*, 97. https://doi.org/10.3847/1538-4357/aabe8b

Moses, J. I. (2014). Chemical kinetics on extrasolar planets. *Philosophical Transactions of the Royal Society of London Series A*, *372*(2014), 20130073. https://doi.org/10.1098/rsta.2013.0073

Moses, J. I., Visscher, C., Fortney, J. J., Showman, A. P., Lewis, N. K., Griffith, C. A., et al. (2011). Disequilibrium carbon, oxygen, and nitrogen chemistry in the atmospheres of HD 189733b and HD 209458b. *Astrophysical Journal*, *737*, 15.

Mousis, O., Ronnet, T., & Lunine, J. I. (2019). Jupiter's formation in the vicinity of the amorphous ice snowline. *Astrophysical Journal*, *875*(1), 9. https://doi.org/10.3847/1538-4357/ab0a72

Niemann, H. B., Atreya, S. K., Carignan, G. R., Donahue, T. M., Haberman, J. A., Harpold, D. N., et al. (1998). The composition of the Jovian atmosphere as determined by the Galileo probe mass spectrometer. *Journal of Geophysical Research*, *103*, 22,831–22,846. https://doi.org/10.1029/98JE01050

Orton, G. S., Fisher, B. M., Baines, K. H., Stewart, S. T., Friedson, A. J., Ortiz, J. L., et al. (1998). Characteristics of the Galileo probe entry site from Earth-based remote sensing observations. *Journal of Geophysical Research*, *103*, 22,791–22,814. https://doi.org/10.1029/98JE02380

Owen, T., Mahaffy, P., Niemann, H. B., Atreya, S., Donahue, T., Bar-Nun, A., & de Pater, I. (1999). A low-temperature origin for the planetesimals that formed Jupiter. *Nature*, *402*, 269–270.

Prinn, R. G., & Barshay, S. S. (1977). Carbon monoxide on Jupiter and implications for atmospheric convection. *Science*, *198*, 1031–1034.

Raymond, S. N., Izidoro, A., & Morbidelli, A. (2018). Solar system formation in the context of extra-solar planets. *arXiv e-prints*, arXiv:1812.01033.

Roos-Serote, M., Vasavada, A. R., Kamp, L., Drossart, P., Irwin, P., Nixon, C., & Carlson, R. W. (2000). Proximate humid and dry regions in Jupiter's atmosphere indicate complex local meteorology. *Nature*, *405*(6783), 158–160. https://doi.org/10.1038/35012023

Strobel, D. F. (1977). NH3 and PH3 photochemistry in the Jovian atmosphere. *Astrophysical Journal Letters*, *214*, L97–L99. https://doi.org/10.1086/182450

Taylor, F. W., Atreya, S. K., Encrenaz, T., Hunten, D. M., Irwin, P. G. J., & Owen, T. C. (2004). The composition of the atmosphere of Jupiter. In F. Bagenal, T. E. Dowling, & W. B. McKinnon (Eds.), *Jupiter. The planet, satellites and magnetosphere* (pp. 59–78). Cambridge: Cambridge University Press.

Tsiganis, K., Gomes, R., Morbidelli, A., & Levison, H. F. (2005). Origin of the orbital architecture of the giant planets of the solar system. *Nature*, *435*(7041), 459–461. https://doi.org/10.1038/nature03539

Venot, O., Cavalié, T., Bounaceur, R., Tremblin, P., Brouillard, L., & Lhoussaine Ben Brahim, R. (2020). New chemical scheme for giant planet thermochemistry. Update of the methanol chemistry and new reduced chemical scheme. *Astronomy & Astrophysics*, *634*, A78. https://doi.org/10.1051/0004-6361/201936697

Venot, O., Hébrard, E., Agúndez, M., Dobrijevic, M., Selsis, F., Hersant, F., et al. (2012). A chemical model for the atmosphere of hot Jupiters. *Astronomy & Astrophysics*, *546*, A43. https://doi.org/10.1051/0004-6361/201219310

Visscher, C., Lodders, K., & Fegley, B. (2006). Atmospheric chemistry in giant planets, brown dwarfs, and low-mass dwarf stars. II. Sulfur and phosphorus. *Astrophysical Journal*, *648*, 1181–1195. https://doi.org/10.1086/506245

Visscher, C., & Moses, J. I. (2011). Quenching of carbon monoxide and methane in the atmospheres of cool brown dwarfs and hot Jupiters. *Astrophysical Journal*, *738*(1), 72. https://doi.org/10.1088/0004-637X/738/1/72

Visscher, C., Moses, J. I., & Saslow, S. A. (2010). The deep water abundance on Jupiter: New constraints from thermochemical kinetics and diffusion modeling. *Icarus*, *209*(2), 602–615. https://doi.org/10.1016/j.icarus.2010.03.029

von Zahn, U., Hunten, D. M., & Lehmacher, G. (1998). Helium in Jupiter's atmosphere: Results from the Galileo probe helium interferometer experiment. *Journal of Geophysical Research*, *103*, 22,815–22,830. https://doi.org/10.1029/98JE00695

Wahl, S. M., Hubbard, W. B., Militzer, B., Guillot, T., Miguel, Y., Movshovitz, N., et al. (2017). Comparing Jupiter interior structure models to Juno gravity measurements and the role of a dilute core. *Geophysical Research Letters*, *44*, 4649–4659. https://doi.org/10.1002/2017GL073160

Wang, D., Gierasch, P. J., Lunine, J. I., & Mousis, O. (2015). New insights on Jupiter's deep water abundance from disequilibrium species. *Icarus*, *250*, 154–164. https://doi.org/10.1016/j.icarus.2014.11.026

Wang, D., Lunine, J. I., & Mousis, O. (2016). Modeling the disequilibrium species for Jupiter and Saturn: Implications for Juno and Saturn entry probe. *Icarus*, *276*, 21–38. https://doi.org/10.1016/j.icarus.2016.04.027

Wong, M. H., Lunine, J. I., Atreya, S. K., Johnson, T., Mahaffy, P. R., Owen, T. C., & Encrenaz, T. (2008). Oxygen and other volatiles in the giant planets and their satellites. *Reviews in Mineralogy and Geochemistry*, *68*(1), 219–246. https://doi.org/10.2138/rmg.2008.68.10

Wong, M. H., Mahaffy, P. R., Atreya, S. K., Niemann, H. B., & Owen, T. C. (2004). Updated Galileo probe mass spectrometer measurements of carbon, oxygen, nitrogen, and sulfur on Jupiter. *Icarus*, *171*, 153–170. https://doi.org/10.1016/j.icarus.2004.04.010